Dependence of superconducting thermodynamics ratios on the shape of the electron-phonon spectral density

J. M. Coombes and J. P. Carbotte
Department of Physics, McMaster University, Hamilton, Ontario, Canada L8S 4M1
(Received 22 October 1987; revised manuscript received 30 June 1988)

We have extended a previous study of the effect of the shape of the electron-phonon spectral density $\alpha^2F(\Omega)$ on the ratio $2\Delta_0/k_BT_c$ to include the thermodynamic indices $\gamma_s[T_c/H_c(0)]^2$, $\Delta C_v/\gamma_s T_c$, and the critical magnetic field deviation $D(t)$. Using realistic shapes, we find small variations which are relatively larger in these ratios than was the case with $2\Delta_0/k_BT_c$. The analysis is extended to a two-δ-function model spectrum to investigate the range of values taken on by these quantities when the shape of $\alpha^2F(\Omega)$ is left relatively unconstrained.

I. INTRODUCTION

In a previous paper[1] we examined the dependence of the ratio of the gap edge Δ_0 to the critical temperature T_c, $2\Delta_0/k_BT_c$, on the shape of the electron-phonon spectral density $\alpha^2F(\Omega)$. To complement this work, we now examine how the shape of $\alpha^2F(\Omega)$, as a function of phonon energy Ω, affects certain thermodynamic properties. We will consider the ratio $\gamma_s[T_c/H_c(0)],^2$ where γ_s is the Sommerfeld constant and $H_c(0)$ the critical magnetic field at zero temperature, the normalized jump in the specific heat at T_c, namely $\Delta C_v(T_c)/\gamma_s T_c$, and the critical-field deviation function $D(t)$ which depends on the reduced temperature $t=T/T_c$.

Such a study clearly cannot be carried out without imposing some constraint on the allowed $\alpha^2F(\Omega)$. This is somewhat arbitrary, and several choices are possible. Here, we follow our previous paper and consider only what we have come to call "realistic" shapes and a more widely varying two-δ-function model to be explained later. The point is the following. We will consider a single system, say Pb, to be definite. Its spectral density is well established from tunneling inversion, as are those of many other metals and alloys including some $A15$ compounds.[2-4] The implied thermodynamics follow from solution of the Eliashberg equations, and the agreement with experiment is good.[5-7] What we want to consider here is the amount by which the calculated thermodynamic properties will be changed as the shape of $\alpha^2F(\Omega)$ is changed in an arbitrary way. As stated, we certainly need to impose some constraints, and to begin we restrict the analysis to other known shapes. At the same time, we want to keep the value of Coulomb pseudopotential, μ^*, and critical temperature fixed to its value in Pb. We could, in addition, insist that the electron-phonon mass renormalization, $\lambda=2\int\{[\alpha^2F(\Omega)]/\Omega\}d\Omega$, remain unchanged as well as some other moments. Here, we fix instead the characteristic phonon energy $\omega_{\ln}$ introduced by Allen and Dynes[8] in their analysis of the critical temperature. The motivation for this is the recent work of Marsiglio and Carbotte[2] which established approximate formulas for the thermodynamic ratios valid for many superconductors. These formulas include a strong-coupling correction of the form $(T_c/\omega_{\ln})^2\ln(\omega_{\ln}/bT_c)$, with b some fixed number. This is taken as an indication that $\omega_{\ln}$ is a significant parameter for characterizing the spectrum. Of course, other moments of $\alpha^2F(\Omega)$ could be important, as is made clear from the fact that the approximate formulas of Marsiglio and Carbotte[2] can, at best, represent only the overall trend in the actual numerical data. In some cases, a particular material can fall considerably off the curve. It is these deviations off the main trend that interest us here.

In a first set of calculations, we consider a variety of measured spectra and rescale them by a linear change on the vertical and horizontal axis. As described by Coombes and Carbotte,[1] this procedure is unique if T_c and $\omega_{\ln}$ are to be chosen to be those for Pb. Such scaled spectra will lead to changes in the thermodynamics which can be taken as a representative measure of how other details of $\alpha^2F(\Omega)$ (other than T_c and $\omega_{\ln}$) can enter the theory. Besides these scaled "realistic" spectra, we will also consider a two-δ-function model which allows us to range over much more of parameter space to include quite extreme unphysical possibilities and to record the variation in thermodynamics that can occur in these cases.

In Sec. II we review some of the basic theory needed, introduce our scaled "realistic" spectra, and present results for $\gamma_s[T_c/H_c(0)]^2$, $\Delta C(T_c)/\gamma_s T_c$, $H_c(0)$ in both tabular and graphical form. The critical magnetic field deviation function, $D(t)$, is also discussed. Section III deals with our two δ function model. Many results are presented and discussed. Finally, in Sec. IV, we draw conclusions.

II. EFFECTS OF SCALING AND RESULTS FOR REALISTIC SHAPES

The Eliashberg equations are fundamental to this work. They give the gap $\tilde{\Delta}_n(T)$ and renormalized Matsubara frequency $\tilde{\omega}_n(T)$ at temperature T as a function of $n=0,\pm1,\pm2$. These depend on the microscopic parameters $\alpha^2F(\Omega)$ and μ^*, the electron-phonon spectral density

and Coulomb pseudopotential, respectively.[7] Once these quantities are known the free-energy difference[9,10] between normal and superconducting state $\Delta F(T)$ can be constructed as a simple sum over the index n. The thermodynamics follows from the free-energy difference in the usual fashion.[7,10]

To start, we reproduce in Figs. 1 and 2 the previous results of Ref. 2, giving the ratios $\gamma_s[T_c/H_c(0)]^2$ and $\Delta C_v/\gamma_s T_c$, respectively, for a very large number of superconductors identified in the caption. The plots are as a function of $T_c/\omega_{\ln}$. While it is clear that $\omega_{\ln}$ is a useful parameter in characterizing these properties, some points do fall off the general trend indicating that aspects of $\alpha^2F(\Omega)$ other than $\omega_{\ln}$ do come into play. These aspects are the topic of this paper.

From here on, we consider the specific case of Pb and start exploring the effects on the thermodynamics of a change in shape of $\alpha^2F(\Omega)$ away from that measured for Pb. Following Ref. 1, we consider several other measured spectra for the spectral density. Denote the measured $\alpha^2F(\Omega)$ for some other material by $\alpha_0^2F(\Omega)$. Next, consider a simple scaling of the vertical and horizontal axes such that the new $\alpha^2F(\Omega)$ is related to the original by

$$\alpha^2F(\Omega)=B\alpha_0^2F(\gamma\Omega)\ ,$$

with B and γ constants. For such a spectrum, we were able to show, in Ref. 1, that $\omega_{\ln}=(1/\gamma)\omega_{\ln}^0$ independent of the vertical axis scaling factor B. Thus γ can be adjusted to get the desired $\omega_{\ln}$ and then B fixed to get the T_c of Pb. The procedure is clear and can now present results.

In Table I we list the material spectra considered and the results of calculations using these spectra as well as the scaling parameters B and γ which are entered in columns 2 and 3. These scaled spectra (which are shown in Ref. 1) vary considerably, with large differences in

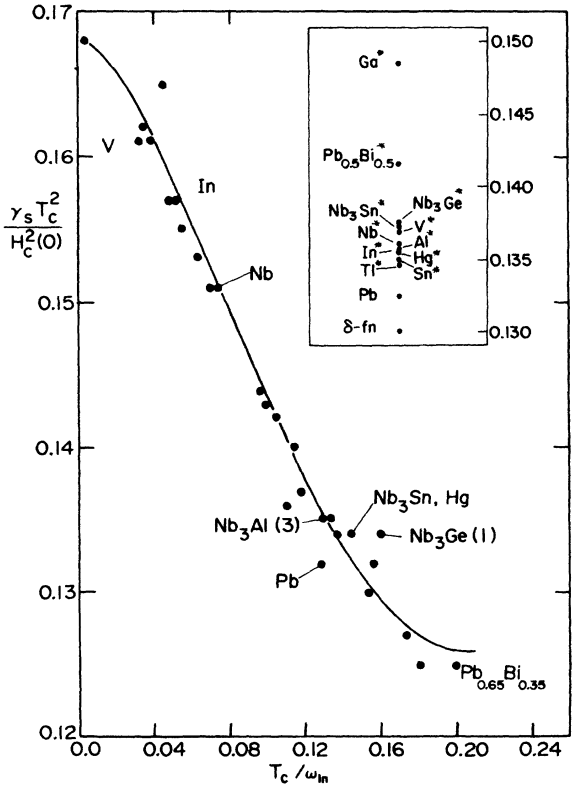

FIG. 1. The ratio $\gamma_s[T_c/H_c(0)]^2$ for a number of superconductors plotted against $T_c/\omega_{\ln}$. The solid dots represent real material results obtained in Ref. 2. In decreasing order of $\gamma[T_c/H_c(0)]^2$, they correspond to the following systems: Al, Tl, Ta, V, Sn, In, $Tl_{0.9}Bi_{0.1}$, Nb (Butler), Nb (Arnold), Nb (Robinson), V_3Si, $Pb_{0.4}Tl_{0.6}$, $Nb_{0.75}Zr_{0.25}$, V_3Ga, Nb_3Al (2), $Pb_{0.6}Tl_{0.4}$, Nb_3Ge (2), $Pb_{0.7}In_{0.3}$, Nb_3Al (3), Nb_3Sn, Hg, Nb_3Ge (1), $Pb_{0.8}Tl_{0.2}$, Pb, Nb_3Al (1), $Pb_{0.9}Bi_{0.1}$, $Pb_{0.8}Bi_{0.2}$, $Pb_{0.7}Bi_{0.3}$, $Pb_{0.65}Bi_{0.35}$. The solid curve corresponds to $\gamma_s[T_c/H_c(0)]^2=0.168[1-12.2(T_c/\omega_{\ln})^2\ln(\omega_{\ln}/3T_c)]$ which is formula (7) in the text. The entries (solid dots) shown in the insert are our scaled realistic spectra results described in the text and Table I.

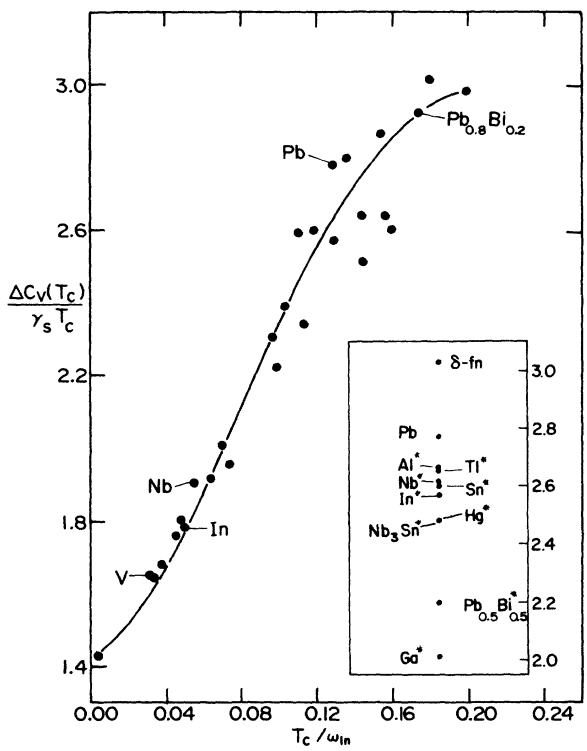

FIG. 2. The ratio $\Delta C_v/\gamma_s T_c$ for a number of superconductors plotted against $T_c/\omega_{\ln}$. The solid dots represent results for real materials obtained in Ref. 2. In increasing order of $\Delta C(T_c)/\gamma_s T_c$, they correspond to the following systems: Al, Ta, V, Sn, Tl, In, $Tl_{0.9}Bi_{0.1}$, Nb (Butler), Nb (Arnold), Nb (Robinson), V_3Si, $Nb_{0.75}Zr_{0.25}$, $Pb_{0.4}Tl_{0.6}$, Nb_3Al (2), V_3Ga, Hg, Nb_3Al (3), Nb_3Ge (2), Nb_3Ge (1), $Pb_{0.6}Tl_{0.4}$, Nb_3Sn, Nb_3Al (1), Pb, $Pb_{0.8}Tl_{0.2}$, $Pb_{0.9}Bi_{0.1}$, $Pb_{0.8}Bi_{0.2}$, $Pb_{0.65}Bi_{0.35}$, $Pb_{0.7}Bi_{0.3}$. The solid curve corresponds to $\Delta C(T_c)/\gamma_s T_c=1.43[1+53(T_c/\omega_{\ln})^2\ln(\omega_{\ln}/3T_c)]$ which is formula (8) in the text. The entries (solid dots) shown in the insert are our scaled realistic spectra results described in the text and Table I.

TABLE I. Details of the various scaled spectra used in Sec. II. They are based on the known values of $\alpha^2F(\Omega)$ for Al, In, Tl, Ga, Nb, V, Sn, $Pb_{0.5}Bi_{0.5}$, Nb_3Sn, Nb_3Ge, and Hg, and for $\alpha^2F(\Omega)$ a δ function. For each scaled spectrum which gives the same T_c and $\omega_{\ln}$ as for Pb, we enter values of the scaling parameters B and γ, the electron-phonon mass enhancement factor λ^*, the area under $\alpha^2F(\Omega)$ (A^*), the maximum, phonon energy ω_D^*, the values of $H_c(0)^*$ (using $N(0)=0.823\times10^{19}$ states/meV cm^3), $\gamma_s[T_c/H_c(0)]^{2*}$), and $\Delta C_v/\gamma_s T_c^*$ and their percent variation off the Pb value, i.e., $(V^*-V^{Pb})/V^{Pb}$. For comparison, we have included the previously published values of $2\Delta_0/k_BT_c$ and its variation.

	B	γ	λ^*	A^* (meV)	ω_D^* (meV)	$H_c(0)$ (Oe)	% diff.	$\gamma_s[T_c/H_c(0)]^2$	% diff.	$\Delta C_v/\gamma_s T_c$	% diff.	$2\Delta_0/k_BT_c$	% diff.
Pb	1	1	1.5477	4.0320	11.0	799.1		0.1324		2.7666		4.4965	
Hg*	0.966	1.957	1.5694	5.0029	28.0	794.6	0.56	0.1350	1.98	2.4817	10.30	4.4890	0.17
Ga*	0.700	1.396	1.5712	6.0035	37.7	758.0	5.15	0.1485	12.18	2.0110	27.31	4.3623	2.98
$Pb_{0.50}Bi^*_{0.50}$	0.557	2.194	1.6700	5.2514	28.7	791.2	1.00	0.1416	6.91	2.2000	20.48	4.4896	0.13
Sn*	2.130	0.575	1.5261	4.1825	10.8	788.1	1.39	0.1349	1.89	2.5979	6.10	4.4617	0.77
In*	1.898	0.828	1.5273	4.3073	13.1	786.9	1.54	0.1355	2.33	2.5667	7.22	4.4517	1.00
Nb_3Ge*	0.943	0.447	1.5084	4.3516	15.4	778.0	2.65	0.1376	3.90	2.4796	10.37	4.4103	1.92
V*	1.877	0.327	1.5040	4.1461	10.8	779.4	2.47	0.1369	3.38	2.5472	7.93	4.4192	1.72
Nb_3Sn*	0.866	0.452	1.5065	4.2791	13.0	778.5	2.58	0.1373	3.66	2.4784	10.42	4.4157	1.80
Al*	3.648	0.199	1.5033	3.9836	8.3	782.8	2.05	0.1356	2.42	2.6653	3.66	4.4399	1.26
Nb*	1.497	0.376	1.5102	4.0831	10.6	782.7	2.06	0.1360	2.72	2.6143	5.50	4.4310	1.46
Tl*	1.925	1.085	1.5303	4.1723	11.8	790.0	1.15	0.1346	1.66	2.6472	4.32	4.4614	0.78
δ-function			1.5649	3.7777	11.0	809.5	1.30	0.1299	1.89	3.0289	9.48	4.5246	0.63

height and in maximum phonon energy ω_D^* (column 6). These variations lead to variations in the electron-phonon mass enhancement factor λ^* [twice the first inverse moment of $\alpha^2F(\Omega)$] and A^* [the area under $\alpha^2F(\Omega)$]. The quantities are entered in columns 4 and 5 of Table I. Although, as we have noted, the spectra themselves vary greatly, the characteristic numbers λ^* and A^* clearly show much less variation. In the next six columns, we give the values for the thermodynamic, $H_c(0)$, $\gamma_s[T_c/H_c(0)]^2$, and $\Delta C_v/\gamma_s T_c$, as well as the present difference of the quantities from the values for Pb. In determining $H_c(0)$, we have used the electronic density of states $N(0)=0.823\times10^{19}$ states/meV cm^3. The thermodynamic ratios, including $D(t)$, are of course independent of $N(0)$. In the last two columns, for comparison, we have entered our previous results for $2\Delta_0/k_BT_c$. Also in Fig. 3, we present the $D(t)$ curves for these scaled spectra. It is clear from these results that compared to $2\Delta_0/k_BT_c$, the thermodynamic quantities are much more sensitive to the differences in the chosen shapes. This is consistent with the work of Marsiglio and Carbotte[2] on a variety of superconductors. These authors state that the visual fit to thermodynamic data using a correction factor of $(T_c/\omega_{\ln})^2\ln(\omega_{\ln}/bT_c)$ is worse than for $2\Delta_0/k_BT_c$. The values of the thermodynamic quantities range from 758.0 Oe to 809.5 Oe for $H_c(0)$, from 0.1299 to 0.1485 for $\gamma_s[T_c/H_c(0)]^2$, and from 2.0110 to 3.0289 for $\Delta C_v/\gamma_s T_c$, while $2\Delta/k_BT_c$ ranges from 4.362 3 to 4.524 6. The variations of $\gamma_s[T_c/H_c(0)]^2$ and $\Delta C_v/\gamma_s T_c$ are shown more clearly in the inserts of Figs. 1 and 2, respectively. Variations in $D(t)$ range from the positive definite function characteristic of Pb to an S-shaped function when Ga* and $Pb_{0.5}Bi^*_{0.5}$ are considered. This last comparison may not be completely fair because both these spectra have considerable weight at low phonon energies, which is characteristic of amorphous metals but not of the crystalline state. If the comparison is restricted only to crystalline spectra, the amount of variation found for $D(t)$ is greatly reduced but is still quite significant. Thus $D(t)$ reflects some of the details of $\alpha^2F(\Omega)$ that go beyond the value of $\omega_{\ln}$ and an overall strength chosen to give the Pb value for T_c. Returning now to Table I, we see that those spectra with A^* [the area under $\alpha^2F(\Omega)$]

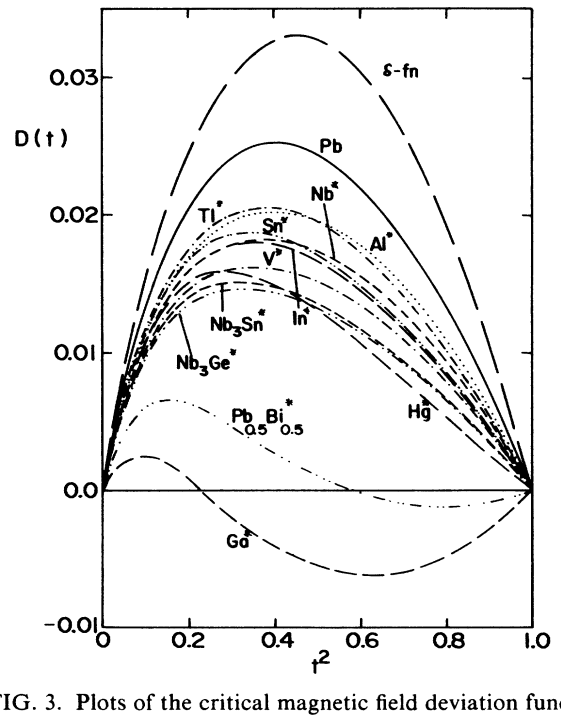

FIG. 3. Plots of the critical magnetic field deviation function $D(t)$ vs the reduced temperature $t=T/T_c$ for the scaled materials listed in Table I. All have the same T_c, μ^*, and $\omega_{\ln}$. The differences come entirely from differences in shape of the spectral density when we use $\alpha^2F(\Omega)=B\alpha_0^2F(\gamma\Omega)$ with $\alpha_0^2F(\Omega)$ the spectral density of the materials described in Table I and B,γ the scaling parameter.

close to that of Pb have much closer thermodynamic values as well. This indicates that the observed variations can be reduced if A^* is additionally constrained to be close to that of Pb. This also applies to our critical-field deviation functions of Fig. 3.

III. A LESS RESTRICTED MODEL

In order to understand better how the shape of the electron-phonon spectral density affects the thermodynamic ratios $\gamma_s[T_c/H_c(0)]^2$, $\Delta C_v/\gamma_s T_c$, and $D(t)$, we next consider model spectra. We start with a single δ function at $\omega_{\ln}$ for Pb. Results for this case have already been presented in the previous section and found to be close to Pb, although the $D(t)$ obtained in this case showed the largest positive deviation of all cases considered. Suppose now that we wish to make a change by moving part of the δ function to higher energy ω_G with $\omega_G > \omega_{\ln}$. To keep $\omega_{\ln}$ invariant, it is necessary to also shift part of the spectral weight to some lower energy $\omega_L < \omega_{\ln}$. Therefore, we need to consider a two-δ-function model of the form

$$\alpha^2F(\Omega) = C[\delta(\Omega-\omega_L)+\bar{B}\delta(\Omega-\omega_G)] , \quad (1)$$

with ω_L and ω_G varied at will within a physically reasonable range. The constants C and $\bar{B}$ are to be determined by the constraints on $\omega_{\ln}$ and T_c.

In Fig. 4(a) we have plotted $\gamma_s[T_c/H_c(0)]^2$ as a function of $\omega_{\ln}/\omega_L$ in the range 1–5 for six different values of $\omega_G/\omega_{\ln}$, namely 1.1, 1.5, 2.0, 4.0, 8.0, and 12.0. In this range of values for ω_L and ω_G, we see that $\gamma_s[T_c/H_c(0)]^2$ ranges from approximately 0.125 (for $\omega_{\ln}/\omega_L = 1.5$ and $\omega_G/\omega_{\ln} = 12.0$) to a maximum value of about 0.176 (for $\omega_G/\omega_{\ln} = 5.0$ and $\omega_G/\omega_{\ln} = 12.0$). Note that the maximum value obtained is larger than the BCS limiting value of 0.168. The two-δ-function model can give larger values than this, but only when there is significant spectral weight at low energies, namely around 1 meV. When this is so, the BCS limit does not apply. The BCS limit only applies when all phonon energies are much greater than the critical temperature. Also, for the cases with significant low-energy spectral weight, the normal state specific heat at T_c can be quite different from $\gamma_s T_c$ because of an important temperature dependence of the electron-phonon renormalization as described by Grimvall.[11,12] Such effects are neglected here, and the zero-temperature Sommerfeld constant has been used rather than the temperature-dependent true value which can be smaller. Note that the range of $\gamma_s[T_c/H_c(0)]^2$ could be increased even further by extending the range of values of $\omega_{\ln}/\omega_L$ and $\omega_G/\omega_{\ln}$. This is unnecessary, since it is very unlikely that we could have in a real material an $\alpha^2F(\Omega)$ exhibiting significant spectral weight outside the range considered. For the convenience of the reader, we show in Fig. 4(b) the same results as we have just presented and discussed but now we have plotted them as a function of $\omega_G/\omega_{\ln}$, namely 1.1, 1.5, 2.0, 3.0, and 5.0. In contrast to the curves in Fig. 4(a) which displayed minima, these new curves display maxima.

In Fig. 5(a) we show our results for $\Delta C_v/\gamma_s T_c$ as a

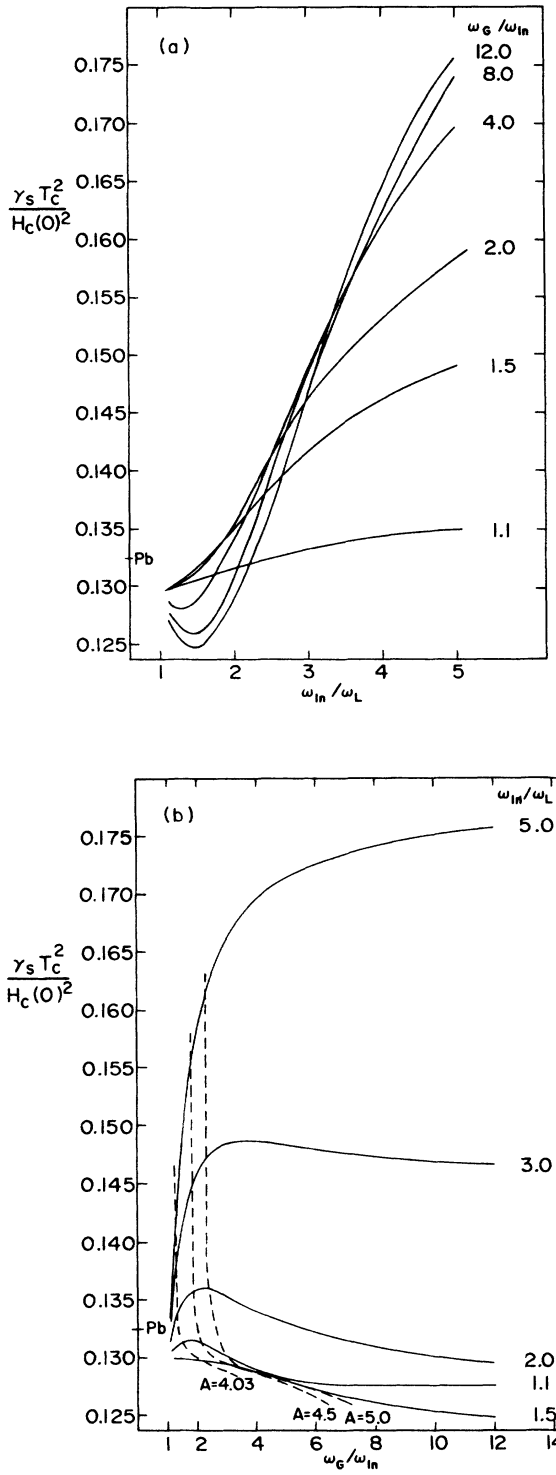

FIG. 4. The thermodynamic ratio $\gamma_s[T_c/H_c(0)]^2$ for our two-δ-function model as a function of choice of ω_L and ω_G, the positions of the two-δ-functions. Here $\omega_L < \omega_{\ln}$ and $\omega_G > \omega_{\ln}$ with $\omega_{\ln}$ fixed. Figure 4(a) gives 6 curves labeled according to $\omega_G/\omega_{\ln} = 1.1$, 1.5, 2.0, 4.0, 8.0, and 12.0 as a function of $\omega_{\ln}/\omega_L$. Figure 4(b) gives the same data and involves five curves labeled by $\omega_{\ln}/\omega_L = 1.1$, 1.5. 2.0, 3.0, and 5.0 as a function of $\omega_G/\omega_{\ln}$. The dashed lines join points on the curves which have the same combined δ function weight, A^* for $A^* = 4.03$ (the Pb value), 4.5, and 5.0.

function of $\omega_{\ln}/\omega_L$ for the same six values of ω_G/ω_L; 1.1, 1.5, 2.0, 2.0, 4.0, 8.0, and 12.0 as previously considered. Again it is clear that if we were willing to go to arbitrarily shaped electron-phonon spectral densities of the two-δ-function type, we could generate an even larger range of values for $\Delta C_v/\gamma_s T_c$. It is seen from the figure that $\Delta C_v/\gamma_s T_c$ can range from approximately 3.10 to 1.19. Again the zero-temperature Sommerfeld constant has been used rather than the temperature-dependent value, and, for this reason, there are values of $\Delta C_v/\gamma_s T_c$ less than the BCS limit of 1.43. The behavior shown by $\Delta C_v/\gamma_s T_c$ is quite similar to the behavior of $\gamma_s[T_c/H_c(0)]^2$ shown in Fig. 4(a), provided one realizes that large values of $\Delta C_v/\gamma_s T_c$ are an indication of strong coupling while the converse is true for $\gamma_s[T_c/H_c(0)]^2$. There are, however, no peaks in $\Delta C_v/\gamma_s T_c$ corresponding to the troughs in $\gamma_s[T_c/H_c(0)]^2$ shown in Fig. 4(a). This is a further indication that these two thermodynamic ratios do not always react to changes in $\alpha^2F(\Omega)$ in the same way. In Fig. 5(b) the same results as just presented are again shown but now $\Delta C_v/\gamma_s T_c$ is plotted against $\omega_G/\omega_{\ln}$ for five values for $\omega_{\ln}/\omega_L$, namely 1.1, 1.5, 2.0, 3.0, and 5.0.

In Fig. 6, $D(t)$ curves for the two-δ-function model are presented to show the range of variation possible under this model along with, for comparison, $D(t)$ for the single δ-function and for real Pb. The first two numbers in brackets refer to the value of $\omega_{\ln}/\omega_L$ and $\omega_G/\omega_{\ln}$, respectively, for the particular $D(t)$ curve. The variation is again large, with large negative values of $D(t)$ possible when there is an unphysical amount of spectral weight around 1 meV. That these $D(t)$ curves are possible can be seen from the functional derivative of $D(t)$.[13] It starts at zero, is negative until a small frequency, and is positive thereafter. The trough can be quite deep compared to the height of the positive region. Recalling that the BCS

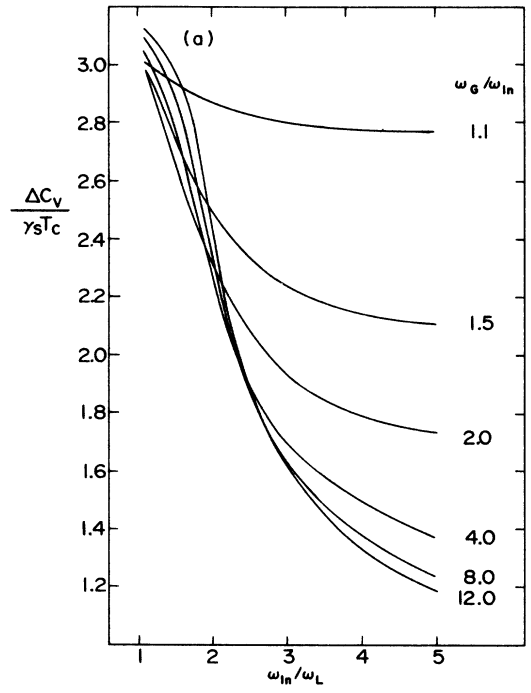

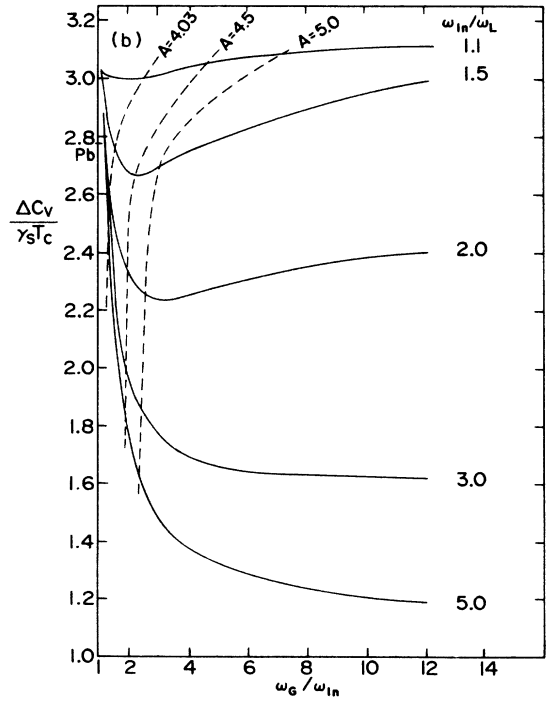

FIG. 5. The same as Fig. 4, but for the specific-heat jump ratio $\Delta C_v/\gamma_s T_c$.

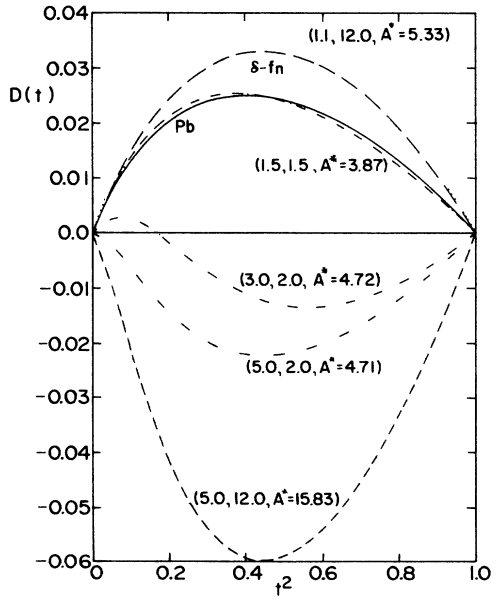

FIG. 6. Plots of the critical magnetic field deviation $D(t)$ vs reduced temperature $t=T/T_c$ for a selection of the two-δ-function models along with Pb and a δ function. The values of $\omega_L/\omega_{\ln}$ and $\omega_G/\omega_{\ln}$ and A are given, respectively, by the numbers in the brackets.

limit applies only for systems with all spectral weight at high frequencies, while the two-δ-function model can have significant weight in the trough, it becomes clear why these large negative $D(t)$ curves appear.

To study the effects of area A as a further constraint on the model, we have in Figs. 4(b) and 5(b) plotted lines illustrating how A changes along the curves. Clearly, as a constraint, A is effective. With $A=4.03$, the Pb value, the range possible for the thermodynamics is reduced, in fact, reduced to a range smaller than the scaled real spectra with unconstrained area. The parameter λ is also constrained, to a range of 1.4–1.6, by fixing A to that of Pb.

IV. CONCLUSIONS

The thermodynamic ratios $\gamma_s[T_c/H_c(0)]^2$, $\Delta C_v/\gamma_s T_c$, and the critical-field deviation function $D(t)$ change when the shape of the electron-phonon spectral density $\alpha^2F(\Omega)$ of Pb is varied, keeping fixed the value of Coulomb repulsion pseudopotential μ^*, the critical temperature T_c, and the characteristic phonon energy $\omega_{\ln}$. Considering first known shapes characteristic of other superconductors, we find considerable variations, much larger than previously found in the case of $2\Delta_0/k_BT_c$. If, however, we further constrain the value of the area under $\alpha^2F(\Omega)$ (A^*) to be near that of Pb the variation is greatly reduced.

To investigate the range of variation in $\gamma_s[T_c/H_c(0)]^2$, $\Delta C_v/\gamma_s T_c$, and $D(t)$ that can be expected if less restricted shapes are considered, we have studied the case of a two-δ-function model centered, respectively, at $\omega_L<\omega_{\ln}$ and $\omega_G>\omega_{\ln}$ with relative weights chosen to preserve the value of $\omega_{\ln}$. For the range of parameters considered, $\gamma_s[T_c/H_c(0)]^2$ varied from 0.125 to 0.176, $\Delta C_v/\gamma_s T_c$ varied from 1.19 to 3.10, and $D(t)$ showed large variations in shape and size from positive definite to S-shaped to negative definite. This clearly indicates that the shape of $\alpha^2F(\Omega)$ is an important ingredient in determining the details of the thermodynamics. On the other hand, it was found that if the area under $\alpha^2F(\Omega)$ is also constrained to a value close to that for Pb, the range of values of ω_L and ω_G is reduced, and the variations in the thermodynamic quantities becomes for $\gamma_s[T_c/H_c(0)]^2$ 0.130 to 0.142 and for $\Delta C_v/\gamma_s T_c$ 2.43 to 3.10. Thus T_c, $\omega_{\ln}$, μ^*, and area A play an important role in defining the thermodynamic ratios of superconductors, although other moments of the spectral density must also enter in some cases.

[1]J. M. Coombes and J. P. Carbotte, J. Low Temp. Phys. **63**, 431 (1986).
[2]F. Marsiglio and J. P. Carbotte, Phys. Rev. B **33**, 6141 (1986).
[3]W. L. McMillan and J. M. Rowell, in *Superconductivity*, edited by R. D. Parks (Marcel Dekker, New York, 1969), Vol. 1, p. 561.
[4]J. M. Rowell, W. L. McMillan and R. C. Dynes (unpublished).
[5]B. Mitrović, E. Schachinger, and J. P. Carbotte, Phys. Rev. B **29**, 6187 (1984).
[6]B. Mitrović, H. G. Zarate, and J. P. Carbotte, Phys. Rev. B **29**, 184 (1984).
[7]J. Daams and J. P. Carbotte, J. Low Temp. Phys. **40**, 135 (1980).
[8]P. B. Allen and R. C. Dynes, Phys. Rev. B **23**, 905 (1965).
[9]J. Bardeen and M. Stephen, Phys. Rev. B **6**, 14 485 (1964).
[10]D. Rainer and Bergmann, J. Low Temp. Phys. **14**, 501 (1974).
[11]G. Grimvall, Phys. Condens. Mater. **9**, 283 (1969).
[12]G. Grimvall, J. Phys. Chem. Solids **29**, 1221 (1968).
[13]J. Daams and J. P. Carbotte, Can. J. Phys. **56**, 1248 (1978).